International Journal of Engineering & Technology, 7 (4.14) (2018) 444-448

International Journal of Engineering & Technology

Website: www.sciencepubco.com/index.php/IJET

Research paper

Interfacial Shear Strength of Kenaf Single Fibre Reinforced Polyester Matrix: Observation of Fibre Fracture and Matrix Debonding

M.N. Zakaria[1]*, A. Crosky[2], A. Beehag[3]

[1]*Faculty of Applied Sciences, Universiti Teknologi MARA, 40450 Shah Alam Selangor, Malaysia*
[2]*School of Materials Science and Engineering, The University of New South Wales, Sydney, NSW 2052 Australia*
[3]*Cooperative Research Centre for Advanced Composite Structures Limited 506 Lorimer Street, Fishermans Bend, Victoria, 3207, Australia*
**Corresponding author E-mail: nazarudin@salam.uitm.edu.my*

Abstract

This paper describes an analysis of the parameters that affect the interfacial properties of kenaf fibre reinforced with polyester matrix. Kenaf fibre bundles were subjected to water treatment through soaking and ultrasonication technique. The specimens of dumbbell shape were fabricated containing kenaf single fibres embedded in polyester matrix. The interfacial shear strength was determined through single fibre fragmentation test. This test was used as a means of investigation, and the observation of fibre fracture and matrix debonding was done using ligt microscope equipped with polarizer light.

Keywords: *kenaf fibre composites, interfacial shear strength, fibre fracture, matrix debonding*

1. Introduction

In recent years, the renewed interest on natural fibre research is giving a new momentum for composites world in investigating the exploitation on these renewable materials due to their specific properties and their clearly positive environmental impact. Many studies have been embarked on the properties of natural fibres as reinforcement in composites since it promises good and realistic alternatives to glass-reinforced composites in many applications [1, 2, 3, 4, 5]. The natural fibres that are most commonly utilised for this application include sisal, jute, flax, kenaf, hemp and cotton [6]. Kenaf is one of the promising materials that provide huge potential for composites application. Its physical and mechanical properties are comparable with other lignocelluloses and agriculture residues. Many studies have reported and revealed on the performance of this fibre in various application. However, there is no or lack of information reporting on the level of adhesion between fibres and matrix interface that ultimately has significant effect on the mechanical properties of a composites. The study on the so called 'interfacial shear strength' has been carried out widely on the synthetic fibre composites, like glass or carbon fibre. Nevertheless, not much research has been undertaken to study the interfacial debonding phenomena on natural fibre composites especially for kenaf fibre. This study has been undertaken to determine and observe the interfacial shear strength and the phenomena of kenaf single fibre fracture in polyester matrix composites.

In order to assess the interfacial shear strength (IFSS) of kenaf single fibre reinforced polyester matrix, the single fibre fragmentation test (SFFT) was carried out as a means of evaluation. This method was chosen because it provides a relatively accurate measurement of the IFSS as the fibre-matrix interface is subjected to pure shear, and the test provides a large amount of data for statistical sampling. In this test, single kenaf fibre or fibre bundles from two different treatments and untreated fibres as a control were used by embedding in polyester resin. Polyester resin which has a sufficient level of transparency with greater strain to failure than the fibre failure strain will ensure full fibre fragmentation beside facilitates the fibre fragments to be observed and measured.

2. Materials and Methods

Long kenaf fibres used for specimen fabrication were supplied by the Malaysian Agricultural Research and Development Institute, MARDI, Malaysia after achieving maturity within 5 months. The kenaf was supplied as bunches with straight long fibres approximately 1200-1500mm in length. The fibres had been separated from their stalks by water retting for about 20 days at MARDI. After the water retting process was complete, the fibres were then cleaned with water and dried under sunlight before being delivered.

2.1. Matrix resin

Clear ESTAREZ® 495P polyester resin with low styrene emission, supplied by Barnes Products Pty Ltd, Australia, was used as the matrix resin for the SFFT specimens. M*ethyl ethyl ketone peroxide* (*MEKP*) was used in the ratio 1:20 *(v/v)* as the hardener, giving a gel time of approximately 13 minutes at 25°C. This allowed sufficient time for resin degassing and alignment of the fibres. The density of the resin at 25°C was 1.11 gcm^{-3} [7].

2.2 Preparation of test specimens

For fibre treatment, the kenaf fibres were treated with tap water by soaking at 100˚C for 4 hours, and by ultrasonication method (SKLON25-12DT Ultrasonic cleaner) at 75ºC for 4 hours using a 60 Watts ultrasonic bath at 50 Hz. Here, the ultrasonication is referred to as 'dynamic treatment' due to the ultrasonic frequency used and soaking is referred to as 'static treatment'. The specimens for the single fibre fragmentation tests were prepared by the method outlined by [8]. The technique involves embedding a single fibre along the centerline of a dog-bone shaped specimen of the matrix material. The dimensions of the specimens used in the present study are shown in Figure 1.

A pattern of the dog bone specimen was first prepared from 2 mm thick timber and a silicone rubber mold then made using the timber pattern. Methyl ethyl ketone peroxide (MEKP) in the ratio 1:10 (v/v) was used as the catalyst for the silicone rubber. The mold was cured overnight at room temperature before being used for casting the specimens.

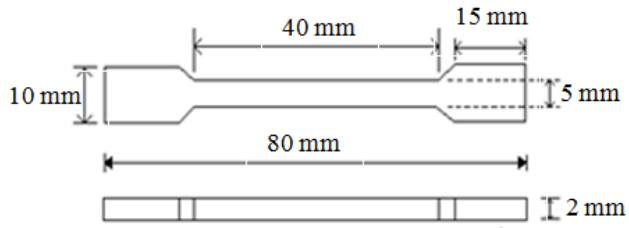

Figure 1: Specimen of dogbone shape for single fibre fragmentation test.

A single fibre was positioned along the centerline of the dogbone cavity in the mold using a special slot incorporated in each end of the mold. The height of the slot was half the specimen thickness, so as to allow the fibre to be positioned in the midplane of the dog bone specimen. Prior to preparation of the specimens, the single fibres were dried at 60 ˚C for 24 hours. Both ends of the single fibre were then lightly prestrained and glued to the mold using cyanoacrylate adhesive. Prestraining is important since the resin shrinks as it cures, and this introduces compressive residual stresses into the fibre which increases the amount of strain required to break the fibre [9]. The polyester resin was mixed, vacuum degassed for 10 minutes, then carefully placed into the mold using a disposable pipette. The specimens were then cured at 80°C for 80 min, then postcured at 100°C for 60 min, then cooled to room temperature in still air.

Prior to examination, each specimen was polished, first using 1200 grade and then using 4000 grade silicon carbide abrasive papers using a Struers polishing machine. This was done to remove the meniscus on the top side of the specimen (which resulted from the open molding process) and also to improve the surface finish so as to improve the visibility of the fibres within the resin dogbone samples. About five specimens were examined for each treated fibre.

2.3 Test apparatus

The specimens were inserted into self-tightening grips faced with a layer of 4000 silicon carbide abrasive paper. Before testing, the average fibre diameter was measured for each specimen at three approximately equally spaced intervals spanning the gauge length of the specimen, using a Nikon ME600 transmitted light microscope fitted with a graduated eye-piece. The specimens were then examined for pre-existing fibre defects such as fibre cracks, voids, and fibre deformation, that were present before the specimens were strained.

Testing was performed using a custom-made Minimat straining rig which was mounted on top of the x-y-stage of the Nikon ME600 microscope. Strain was applied manually by rotating a 100 mm diameter drive wheel. The rig was calibrated prior to testing by measuring the displacement produced per revolution of the drive wheel. The specimens were viewed using polarized light to allow imaging of fibre breaks and the stress field in the matrix. The specimens were slowly loaded axially in increments of 0.25% strain and the number of breaks along the fibre recorded as a function of increa ing strain. Loading was continued until either full fragmentation had occurred (saturation) or the specimen broke. The location of each fibre break in the specimen was recorded as a digital image, after unloading the specimen to enable the fragment lengths to be determined. Interfacial shear strength (τ) was calculated using the equation [10]:

$$\tau = \frac{\sigma_{fu} d}{2 l_c} \quad (1)$$

where d is the diameter of the fibre, l_c is the critical fibre length, and σ_{fu} is the fibre strength at the critical fibre length. The critical fibre length was estimated following the analysis of Oshawa et al. [11] using the equation:

$$l_c = \frac{4}{3}\bar{l} \quad (2)$$

where $\bar{l}$ is the average fragment length. The fibre strength at the critical fibre length, l_c was extrapolated from the single fibre tensile test results given in [12] using the Weibull weakest link rule according to the relationship:

$$\frac{\sigma l_c}{\sigma l_1} = \left(\frac{l_1}{l_c}\right)^{\frac{1}{m}} \quad (3)$$

where l_1 is the fibre length at which the single fibre testing was carried out (20 mm) and m is the experimentally determined Weibull modulus given elsewhere [12].

3. Results and discussions

3.1. Observation of photoelastic features

Figure 2 shows a SFFT specimen before testing, viewed under (a) white light and (b) polarised light illumination. Defects are clearly visible as white bands traversing the fibres in the polarised light images but these are less readily visible in the white light image. Figure 3 shows the typical progression of fibre breakage in the SFFT specimens. The matrix is essentially uniform in appearance at zero loading, Figure 3(a), but birefringence patterns are evident in the vicinity of fibre breaks in Figures 3 (b) and (c). However, the birefringence is absent at the fibre breaks.

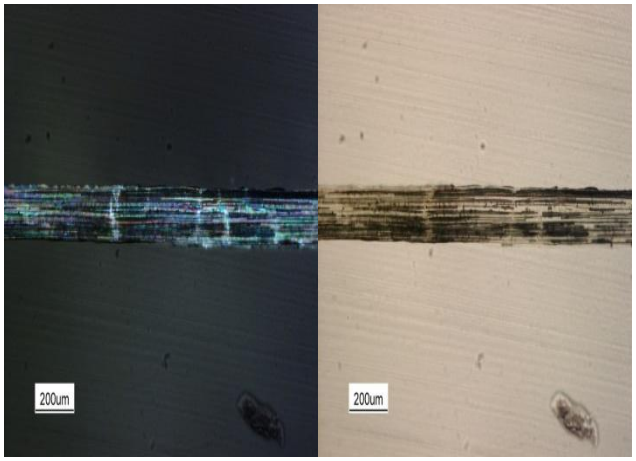

(a) (b)

Figure 2: Micro-compressive failure in single kenaf fibre (a) viewed under diascopic simplified polarization mode (5x magnification) (b) unpolarised white light (5x magnification).

Figures 4 (a) and (b) show a fibre break at higher magnification. It can be seen that the zone over which the birefringence is absent is longer than separation of the broken ends of the fibre and this is attributed to debonding at the fibre-matrix interface in the vicinity of the break [13]. The debonded zone adjacent to a fibre break in a glass fibre SFFT specimens shown for comparison in Figure 4 (c).

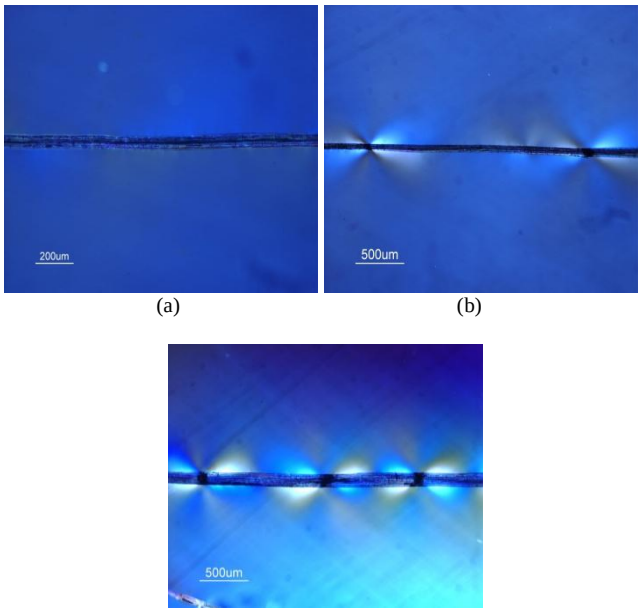

(a) (b)

(c)

Figure 3: Photoelastic birefringence of stress around a fiber break of single kenaf fibre composites with all viewed under x5 magnification (a) under zero loading condition (b) two fibre breaks (c) multiple fibre breaks.

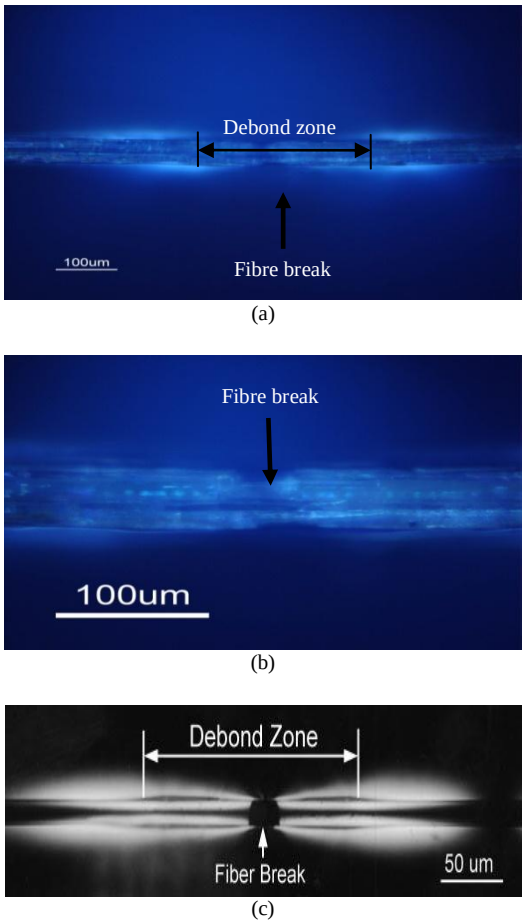

(a)

(b)

(c)

Figure 4: The fiber break of single kenaf fibre and single glass fiber composites specimen during tensile test viewed under diascopic simplified polarization mode (a) 20x magnification (b) 50x magnification (c) single glass fiber composites [13].

3.2. Fibre breaks

Figure 5 shows an SFFT specimen loaded to saturation. Separation of the broken ends is clearly visible. In addition, the fragments can be seen to be of different lengths as observed across the specimens. The variation in fragment length is due to the statistical distribution of defects in the fibres. The first break occurs at the most severe defect (i.e., at the weakest point) with progressively less severe defects causing failure as the load increases. As noted earlier, eventually the fragments become too short for sufficient load to break the fibre being transferred into the fibre through the interface by shear and saturation occurs. Figure 6 shows examples of the defects present in the single fibres in the SFFT specimens.

Strain concentration at the ends of fibre fractures can also lead to crack initiation within the matrix due [14]. Figure 7 shows a small crack in the matrix. Such cracks could ultimately lead to macroscopic fracture of a composite. While the results of the present study are similar to those observed for synthetic fibre composites, it is noted that the single fibres used in most synthetic fibre studies were single filaments whereas the fibres used in the present study were fibre bundles. As can be seen in Figure 6, defects in the kenaf fibres often span several of the individual elementary fibres in the single fibre bundles but do not always traverse the entire bundle.

Moon and Mcdonough [15] examined the effect of fracture of a single fibre on the adjacent fibres in multiple fibre E-glass/polyisocyanurate fragmentation specimens with varying interfibre spacing. It was found that there was no interaction between the fibres for interfibre spacings of >200 µm but at smaller spacings fracture of one fibre caused in-line fracture of its neighbours. This suggests that for the kenaf fibre bundles, in which the individual elementaries are very closely spaced, the defects will initiate failure of the entire bundle even when they do not span the entire bundle.

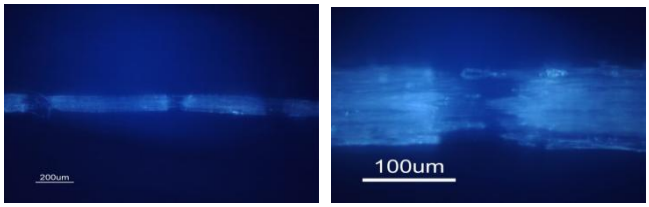

(a) (b)

Figure 5: Typical fibre fracture in SFFT of kenaf fibre viewed under Episcopic simplified polarization mode (a) 10x magnification and (b) 50x magnification

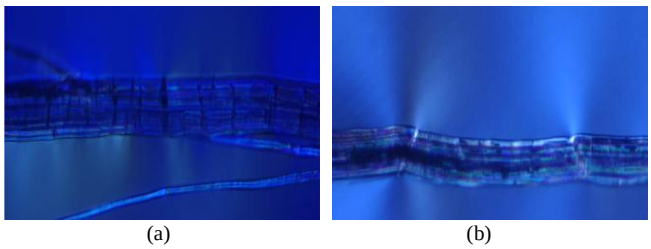

(a) (b)

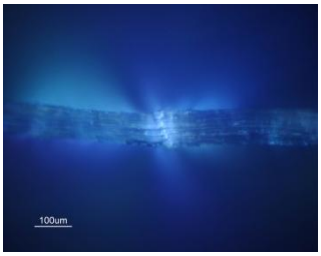

(c)

Figure 6 Micro-compressive defect and damage present in kenaf fibre, embedded in polyester matrix (a) micro compressive damage (b) kink bands (c) micro-compressive defect.

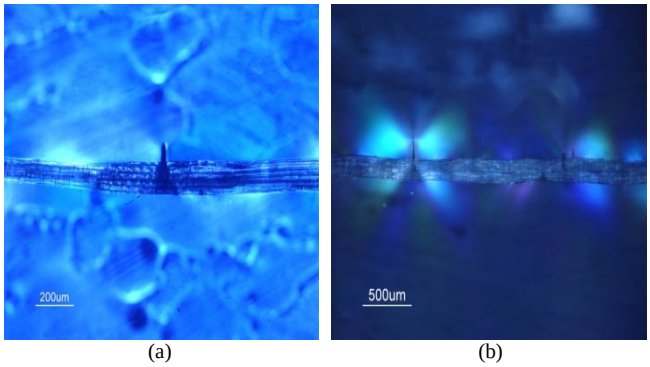

(a) (b)

Figure 7: Formation of matrix cracks in a failed kenaf single fibre reinforced polyester matrix (a) diascopic simplified polarization mode (x5 magnification) (b) diascopic simplified polarization mode (x5 magnification).

3.3. Interfacial shear strength

The fragmentation profiles obtained from the average no of fibre breaks at each increment of strain are shown for the three treatments in Figure 8. All have an essentially S-shaped form, as has been reported previously for glass and carbon fibres [13]. Initial fibre breakage started at strains of 1.0-1.25% for all three treatments. For the untreated fibres, the number of breaks increased slowly up to a strain of 1.5%. The number of breaks then increased rapidly, but then plateaued over the strain range 2.5% to 3.75%. After that the number of breaks increased again up to a strain of 4.25%, where after no further change occurred.

In contrast, for the soaked fibres, the number of breaks remained constant up to a strain of 2% strain, but thereafter increased rapidly. This was followed by a reduction in the rate of increase beyond a strain of 3%, with a plateau occurring at 4.25%. The behaviour for the ultrasonicated fibres was intermediate between that for the untreated fibres and that for the soaked fibres. As for the untreated fibres, there was a gradual increase in the number of breaks in the low strain range followed by a rapid increase at higher strain. However, the rapid increase did not commence until a much higher

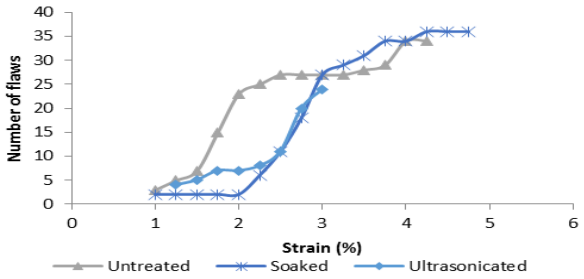

Figure 8: Fragmentation profile for kenaf single fibre reinforce polyester matrix in fragmentation test (SFFT).

Table 1: Summary of the results obtained from the single-fibre fragmentation test of kenaf single fibres reinforced polyester matrix and different types of natural fibres.

Fiber Types	d (μm)	$\bar{l}$ (μm)	l_c (μm)	σ_{fu} (MPa)	τ(MPa)
Untreated	75.66	1866.07	2488.1	595.83	9.1
Ultrasonicated	120.63	1939.88	2586.5	570.05	13.3
Soaked	109.15	1233.28	1644.4	1226.03	40.7
Untreated Jute Filament*	-	500	670	2455	83
Silver Jute Filament*	-	400	530	1430	58
Bleached Jute Filament*	-	420	560	3455	140
Mercerized Jute Filament*	-	430	570	1200	47
5% NaOH/1% DGEBA treated fiber (PALFs)**	39.8	290	390	1420	72.40
Untreated kenaf fiber ***	Pullout technique on kenaf fiber bundle				10

Key:
d, $\bar{l}$, l_c, σ_{fu}, and τ are fiber diameter, average fiber fragment length, critical fiber length, fiber strength at critical fiber length, and interfacial shear strength (*16, ** 17,***18).

strain value (2.25%) than was observed for the untreated fibres. At this point the curve then became synonymous with that for the soaked fibres.

The slope of the steepest part of the curve (i.e., rate of breakage per increment of strain) was the same for all three treatments, though this region of the curve occurred at a higher strain for the soaked and ultrasonicated fibres than for the untreated fibres. The results obtained from the fragmentation tests are given in Table 1. The soaked fibres gave the highest value of interfacial shear strength of 40.7 MPa, with a value of 13.3 MPa being obtained for the ultrasonicated fibres, and 9.1 MPa for the untreated fibres. The better shear strength for the hot water treated fibres, and its increase with the temperature of hot water treatment, are considered to be due to the progressive removal of waxes and pectins from the fibre surface, as indicated by the FTIR results given in Section 4.3.1 and the correspondingly increasingly cleaner fibre surfaces seen by SEM examination, Section 3.3.4. The cleaner fibre surface would allow better mechanical anchorage of the matrix resin to the fibres [16].

Data is also given in Table 1 from previous studies of treated and untreated jute [16], treated pineapple leaf [17], and untreated kenaf [18]. The interfacial shear strengths obtained in the present study are within the range reported from these previous studies. The interfacial shear strength of 10 MPa determined by Park et al. [18] for untreated kenaf fibre, using the pullout technique, is very close to the value of 9.1 MPa obtained for untreated fibres in the present study.

4. Conclusion

Photoelasticity birefringence pattern under polarized light was found to be of great tool in determining the fibre damage or broken fibre in single fibre fragmentation test. In this study, the fibre start to break once it reached the maximum tensile strength and it can be observed by birefringence colours near the vicinity of the fibre breaks which represent shear stress originated from the tensile loading. The saturation state reached when the fragment length is so small that the applied tensile stress can no longer reach the strength of that fragment. The failure mechanism was either fibre break or interfacial debonding which results in different stress-birefringent pattern. For fibre break, the shear stress was scattered near the fibre break with the birefringence symmetrically featured at both sides of the fibre break. Meanwhile for interfacial debonding, the stress birefringence patterns slightly longer and flatter for higher strain. Generally, the single kenaf fibre does not break into the fragments of equal size, otherwise a wide variation in fragment lengths was observed. The interfacial shear strength determined from the fragmentation test was 40.7 MPa for the soaked fibres, 13.3 MPa for the ultrasonicated fibres and 9.1 MPa for the untreated fibres. The improvement of interfacial shear strength with temperature of hot water treatment is attributed to the progressive removal of pectins and waxes from the surface of the fibres resulting in improved fibre matrix bonding. Crack initiation in the matrix was sometimes seen at the point of fibre fractures. This has been reported previously and is attributed to strain concentration at the fibre fracture.

Acknowledgement

This research was undertaken as part of the research program of the Cooperative Research Centre for Advanced Composite Structures Ltd. Victoria, Australia and Universiti Teknologi MARA, Malaysia. Thank you to Malaysian Agricultural Research and Development Institute, MARDI, Malaysia for kenaf supplied.

References

[1] Bledzki, A.K. and Gassan, J. (1999), Composites reinforced with cellulose based fibres, *Progress in Polymer Science, 24*: 221–274.

[2] Eichhorn, S.J., Baillie, C. A., Zafeiropoulos, N., Mwaikambo, L.Y, Ansell, M. P., Dufresne, A., Entwistle, K. M., Herrera-Franco, P. J., Escamilla, G. C., Groom, L., Hughes, M., Hill, C., Rials, T. G. and Wild, P.M. (2001), Review current international research into cellulosic fibres and composites. *Journal of Materials Science 36*; pp. 2107 – 2131.

[3] Joshi, S.V., Drzal, L.T., Mohantyb, A.K. and Arora, S. (2004), Are natural fibre composites environmentally superior to glass fibre reinforced composites? *Composites: Part A 35*; pp. 371–376.

[4] Mohanty, A. K., Misra, M. and Hinrichsen, G. (2000), Biofibres, biodegradable polymers and biocomposites: An overview, *Macromolecular Materials and Engineering, 276/277*; pp. 1–24.

[5] Zampaloni, M., Pourboghrat, F., Yankovich, S. A., Rodgers, B. N., Moore, J., Drzal, L. T., Mohanty, A. K. and Misra, M. (2007), Kenaf natural fibre reinforced polypropylene composites: A discussion on manufacturing problems and solutions, *Composites: Part A (Applied science and manufacturing) 38*; pp. 1569–1580.

[6] Robson, D., Hague, J., Newman, G., Jeronomidis, G. and Ansell, M. (1996) Survey of Natural Materials for Use in Structural Composites as Reinforcement and Matrices*" (Woodland Publishing Ltd, Abingdon).*

[7] Barnes (2010) Technical Data Sheet for ESTAREZ®495P Polyester Resin. www.barnes.com.au.

[8] Herrera-Franco and Drzal (1992), Comparison of methods for the measure ment of fibre/matrix adhesion in composites. *Composites Volume 23, Number 1*: pp. 2-27.

[9] Feih,S., Wonsyld, K., Minzari, D., Westermann, P. and Lilholt, H. (2004) Testing procedure for the single fiberfragmentation test. *Risø National Laboratory Roskilde Denmark.*

[10] Kelly, A. and Tyson, W. R. (1965), Tensile properties of fibre-reinforced metals: copper/tungsten and copper/molybdenum, *J Mech Phys Sol 13*: pp. 329–350.

[11] Oshawa, T., Nakayama, A., Miwa, M. and Hasegawa, A. (1978), Temperature dependence of critical fibre length for glass fibre reinforced thermosetting resins, *J. Appl. Polym. Sci. 22*: pp. 3203–3212.

[12] Zakaria, M. N. (2013), Characterization of Kenaf Bast Fibres and their Behaviour as Reinforcement in Polyester Matrix Composites. PhD Thesis, University of New South Wales, Sydney, Australia.

[13] Kim, B. W. and Nairn, J. A. (2002), Observations of Fiber Fracture and Interfacial Debonding Phenomena Using the Fragmentation Test in Single Fiber Composites. *Journal of Composite Materials, 36*: pp. 1825-1858.

[14] Hughes, J. M., Sebe, G., Hague, J., Hill, C., Spear, M. and Mott, L. (2000) An investigation into the effects of micro-compressive defects on interphase behaviour in hemp-epoxy composites using half-fringe photoelasticity. *Compos. Interface., 7 (1)*, 13-29.

[15] Moon, C. K. and McDonough, W. G. (1998), Multiple fiber technique for the single fiber fragmentation test. *Journal of Applied Polymer Science, Vol. 67, Issue 10*: Pp. 1701-1709.

[16] Tripathy, S. S., Landro, L. D., Fontanelli, D., Marchetti, A. and Levita, G. (2000), Mechanical Properties of Jute Fibers and Interface Strength with an Epoxy Resin. *Journal of Applied Polymer Science, Vol. 75*: Pp. 1585–1596.

[17] Lopattananon, N., Payae, Y. and Seadan, M. (2008) Influence of Fiber Modification on Interfacial Adhesion and Mechanical Properties of Pineapple Leaf Fiber-Epoxy Composites. *Journal of Applied Polymer Science, Vol. 110*: Pp. 433–443.

[18] Park, J. M., Quang, S. T, Jung, J. G. and Hwang, B. S. (2006) Interfacial evaluation of single Ramie and Kenaf fiber/epoxy resin composites using micromechanical test and nondestructive acoustic emission. *Composite Interface, Vol. 13, No. 2-3,* pp. 105-129.